38894-54-1; diphosFe$_2$(CO)$_8$, 39022-97-4; diphosFe(CO)$_3$, 38894-55-2.

Acknowledgments. W. R. C. and J. R. S. are grateful to the National Research Council of Canada for financial support. J. R. S. also thanks the Royal Society for the award of a bursary. M. G. C. gratefully acknowledges the financial support provided by a fellowship of St. John's College, Cambridge. Dr. D. B. Patterson is thanked for a helpful discussion.

Contribution No. 4465 from the Arthur Amos Noyes Laboratory of Chemical Physics, California Institute of Technology, Pasadena, California 91109, and Contribution from the Los Alamos Scientific Laboratory, University of California, Los Alamos, New Mexico 87544

Potential Constants of Manganese Pentacarbonyl Bromide from the Vibrational Spectra of Isotopic Species[1]

DAVID K. OTTESEN,* HARRY B. GRAY, LLEWELLYN H. JONES, and MAXWELL GOLDBLATT

Received July 31, 1972

Infrared and Raman spectra are reported for Mn(^{12}C^{16}O)$_5$Br, Mn(^{13}C^{16}O)$_5$Br, and Mn(^{12}C^{18}O)$_5$Br as solids and in CH_2Cl_2 solutions. Most of the fundamental vibrations have been definitively assigned. Compliance constants with standard deviations and their equivalent force constants have been calculated for a general quadratic valence potential field. Changes in the σ- and π-bonding systems in going from Cr(CO)$_6$ to Mn(CO)$_5$Br are deduced by a detailed examination of the internal valence potential constants.

Introduction

The present paper seeks to establish the transferability of the general quadratic potential field calculated for M(CO)$_6$[2] to Mn(CO)$_5$Br. Although the use of ^{13}CO and C^{18}O would be expected to aid considerably in the calculations, the lowering of symmetry from O_h to C_{4v} is so great that a large number of potential constants must be constrained in the calculation. In order to establish suitable constraints one must rely upon information from other systems, such as M(CO)$_6$.

Apart from the question of transferability, the complete normal-coordinate calculation for Mn(CO)$_5$Br is of considerable interest due to the very large number of partial vibrational analyses in recent years on M(CO)$_5$L systems. Almost all of these investigations have been concerned with elucidating the nature of the M–L bond by characterizing the CO stretching frequencies within an "energy-factored" CO force field.

The simplest and by far most heavily used approach is that due to Cotton and Kraihanzel[3] (C-K) which involves the relations between cis and trans CO,C′O′ interaction constants based on a π-bonding model. Many of the investigators using the C-K field have carefully mentioned the inherent approximations, and yet the ordering of a large number of ligands as to π-acceptor or π-donor ability has been widely accepted with little questioning of the effects of possible electrostatic interactions or changes in the σ-bonding system.[4] Such π-bonding orderings must be eyed with suspicion in view of the calculation of Jones, *et al.*,[2] who showed that the relations in the C-K field do not compare well at all with the values for the M(CO)$_6$ harmonic, general quadratic valence potential field.

It should be noted that the present calculation is based on a compliance field although force constants are also presented. The use of compliance constants in vibrational analyses is more fully described in previous papers.[5,6] Their chief advantage over force constants in the present calculation lies in the more complete description of the potential constants involving internal coordinates leading to redundant symmetry coordinates (*i.e.*, the CMC and CMX angle bending).

Experimental Section

Synthesis of Enriched Mn(CO)$_5$Br Species. The normal, ^{13}CO, and C^{18}O species were prepared by the reaction[7] of Mn$_2$(CO)$_{10}$ with Br$_2$ in CCl$_4$ solution. Normal Mn$_2$(CO)$_{10}$ was obtained from Alfa Inorganics and the enriched species were prepared by the reaction of manganese acetate in isopropyl ether with enriched CO under pressure.

Carbon monoxide enriched to 93% ^{13}C was obtained from Mound Laboratory of Monsanto Research Corp., Miamisburg, Ohio. The oxygen-enriched carbon monoxide contained 99% ^{18}O and was prepared from ^{15}N^{18}O as described earlier.[2]

The purity of each compound was checked by comparison of the CO stretching frequencies with those of normal Mn(CO)$_5$Br.[8] The pattern of the primary absorptions for the enriched species is similar to the spectrum of the normal compound but is shifted to lower energy. By using this spectral comparative method sufficient reaction of the Mn$_2$(CO)$_{10}$ was guaranteed, and any impurity of Mn$_2$(CO)$_8$Br$_2$ could be detected and removed by recrystallization.

Observation of Spectra. The Raman spectra were obtained for the solids and solutions on a Cary 81 with a Spectra-Physics Model 125 He–Ne laser source. Solid-state Raman spectra were obtained from powders, and the solution spectra were obtained with CH_2Cl_2 as solvent. The CH_2Cl_2 solutions were contained in glass capillary tubes; laser power at the capillary was 25 mW. No decomposition of the solutions was noticed over the period of observation (about 1 hr at most). The observation of so few Raman lines for concentrated CH_2Cl_2 solutions in contrast to the powder spectra is attributed to solubility limitations and pronounced solvent line broadening. Slit widths were typically 3–5 cm^{-1} with very high

* To whom correspondence should be addressed at Sandia Laboratories, P.O. Box 969, Livermore, Calif. 94550.

(1) This work was sponsored in part by the U. S. Atomic Energy Commission.

(2) L. H. Jones, R. S. MacDowell, and M. Goldblatt, *Inorg. Chem.*, 8, 2349 (1969).

(3) F. A. Cotton and C. S. Kraihanzel, *J. Amer. Chem. Soc.*, 84, 4432 (1962).

(4) Recently Graham has attempted to consider possible σ-bonding effects in M(CO)$_5$L systems; unfortunately these calculations incorporate the ratios assumed for the C-K force field: W. A. G. Graham, *Inorg. Chem.*, 7, 315 (1968).

(5) L. H. Jones, *J. Mol. Spectrosc.*, 36, 398 (1970).

(6) (a) J. C. Decius, *J. Chem. Phys.*, 38, 241 (1963); (b) L. H. Jones and R. R. Ryan, *ibid.*, 52, 2003 (1970).

(7) E. W. Abel and G. Wilkinson, *J. Chem. Soc.*, 1501 (1959).

(8) H. D. Kaesz, R. Bau, D. Hendrickson, and J. M. Smith, *J. Amer. Chem. Soc.*, 89, 2844 (1967).

Table I. Observed Infrared and Raman Fundamental Frequencies of $Mn(CO)_5Br$

Assignment	$Mn(^{12}C^{16}O)_5Br$			$Mn(^{13}C^{16}O)_5Br$			$Mn(^{12}C^{18}O)_5Br$		
	Ir	Raman		Ir	Raman		Ir	Raman	
	CH_2Cl_2 soln	CH_2Cl_2 soln[b]	Solid[c]	CH_2Cl_2 soln	CH_2Cl_2 soln[b]	Solid[c]	CH_2Cl_2 soln	CH_2Cl_2 soln[b]	Solid[c]
ν_1	2137.9	2137.7 p		2088.9	2088.2 p		2090.6	2090.6 p	
ν_9		2085.4 dp			2038.3 dp			2038.1 dp	
ν_{15}	2052.2			2007.0			2004.0		
ν_2	2007.3	2007.0 dp		1962.6	1962.0 dp		1961.8	1962.0 dp	
ν_3	645.0 sh		647.4	632.0 sh		634.2	641.3 sh		644.0
ν_{16}	638.4		635.4	622.0		624.2	636.2		632.2
ν_{10}			626.8			613.4			623.2
ν_{17}	545.5		~546	527.1		~528	542.8		~544
ν_{13}			537.4			517.4			534.7
ν_4		470.4 p	473.2		462.3 p	464.5		459.8 p	462.1
ν_{11}			427.1			418.5			410.1
ν_{18}	417.2		414.3	411.7		407.7	411.2		407.2
ν_{19}	408.5			396.8			402.7		
ν_5		380.5 p	383.9		374.8 p	378.1		366.5 p	370.4
ν_6		222.4 p	218.5		221.6 p	217.4		220.6 p	216.6
ν_{20}	133[a]								
	122[a]		124.3			123.1			116.9
ν_{14}			129.6			128.6			122.8
ν_7	115[a]		115.8			114.0			109.9
ν_{12}			99.0			98.5			95.6
	102[a]								
ν_{21}	87[a]								
ν_{22}	52[a]		52.9			52.5			51.0

[a] These values are from the solid-state Nujol mull spectrum. Accuracy is ±1 cm^{-1}; only normal species are observed due to the large amount of material required. [b] Polarization data for Raman solution spectra are indicated by p or dp. [c] Raman spectra of the CO stretching region in the solid state are reported: I. S. Butler and H. K. Spendjian, *Can. J. Chem.*, 47, 4117 (1969); I. J. Hyams and E. R. Lippincott, *Spectrochim. Acta, Part A*, 25, 1845 (1969). This spectral region was not recorded for the solid-state isotopic species.

amplifier sensitivity. Reproducibility of moderate to strong bands was usually within ±0.3 cm^{-1} and always less than ±0.7 cm^{-1}. The instrument was calibrated within ±0.2 cm^{-1} by means of several lines of the Ne gas emission spectrum.[9]

The infrared spectra of CH_2Cl_2 solutions and KBr pressed disks were obtained on Perkin-Elmer 225 and 521 instruments. The CH_2Cl_2 solutions were contained in KBr cells. The range was 2800–200 cm^{-1} and the reproducibility of most bands was less than ±0.3 cm^{-1}. Calibrations were made from vibrational-rotational spectra of several gases[9] and from the pure rotational spectrum of water vapor.[10] Low-energy infrared measurements were made on Nujol mulls of only the normal species because the large amount of material required was not available for the isotopic species. A Beckman IR-11 spectrometer with an accuracy of ±1 cm^{-1} was employed in the range 250–33 cm^{-1}. Resolution of shoulders and overlapping peaks was accomplished by assuming gaussian band shapes.

Results

The infrared and Raman spectra from 2200 to 50 cm^{-1} are illustrated in Figure 1 for the normal species. The observed infrared and Raman frequencies of the isotopic species in solution are reported in Table I with their Raman polarizations (where observed). Also in Table I are values for the Raman spectra (and infrared data from 200 to 33 cm^{-1}) of the compounds in the solid phase, as many of the weaker bands were not observed for the CH_2Cl_2 solutions.

Anharmonic corrections and the harmonic frequencies, ω_i, have been previously reported[11] for the CO stretching modes of the normal species; the ω_i are listed with those for the isotopic species in Table II. The latter values were calculated from the expression $X^{(i)}_{kl} = X^{(i)}_{kl}\omega^{(i)}_k\omega^{(i)}_l/\omega^{(j)}_k\omega^{(j)}_l$ where X is the anharmonic correction and ω is the harmonic frequency; the superscripts indicate the isotopic species, and the subscripts refer to the normal modes involved.[12]

Table II. Observed and Harmonic CO Stretching Frequencies

ω	$Mn(^{12}C^{16}O)_5Br$		$Mn(^{13}C^{16}O)_5Br$		$Mn(^{12}C^{18}O)_5Br$	
	Obsd	Harmon	Obsd	Harmon	Obsd	Harmon
ω_1	2137.9	2158.7	2088.6	2108.2	2090.6	2110.6
ω_9	2085.4	2083.8	2038.3	2036.7	2038.1	2036.5
ω_{15}	2052.2	2078.5	2007.0	2032.8	2004.0	2029.6
ω_2	2001.3	2030.8	1962.3	1984.0	1961.9	1985.0

Lattice Field Splittings. For interpretation of the solid-state results it is useful to know the perturbations expected by lattice coupling. The crystal structure of $Mn(CO)_5Br$ has been studied by Greene and Bryan.[13] They assigned the space group P_{nma} (D_{2h}^{16}) with the molecules on C_s sites [isomorphous with $Mn(CO)_5Cl$].

Under the unit cell group each A_1 and B_2 mode gives two Raman-active and two infrared-active modes, which may exhibit correlation field splitting. Similarly, each A_2 and B_1 mode gives two Raman-active modes and only one infrared-active mode, again subject to correlation field splitting. The E modes may be split into static field doublets on the C_s site. These may suffer further correlation field splitting into a total of four Raman-active and three infrared-active modes. We may expect site splitting to be considerably greater than correlation field splitting for neutral species such as $Mn(CO)_5Br$ and in this approximation only the E modes would show splitting (into two modes, each infrared and Raman active).

Fundamental Frequency Assignments. Frequency assignments are listed in Table I, while internal coordinates are illustrated in Figure 2 and symmetry coordinates are listed in Table III.

The Region 2200–1900 cm^{-1}. The CO stretching region

(9) IUPAC Commission on Molecular Structure and Spectroscopy, "Tables of Wavenumbers for the Calibration of Infrared Spectrometers," Butterworths, London, 1961.

(10) K. N. Rao, C. J. Humphreys, and D. H. Rank, "Wavelength Standards in the Infrared," Academic Press, New York, N. Y., 1966.

(11) L. H. Jones, *Inorg. Chem.*, 7, 1681 (1968).

(12) G. Herzberg, "Infrared and Raman Spectra," Van Nostrand, Princeton, N. J., 1945.

(13) P. T. Greene and R. F. Bryan, *J. Chem. Soc. A*, 1560 (1971).

Table III. Internal Symmetry Coordinates for $Mn(CO)_5Br$

$$A_1\begin{cases} S_1 = {}^1/_2(R_1 + R_2 + R_3 + R_4) \\ S_2 = R_{ax} \\ S_3 = {}^1/_2(\gamma_1 + \gamma_2 + \gamma_3 + \gamma_4) \\ S_4 = D_{ax} \\ S_5 = {}^1/_2(D_1 + D_2 + D_3 + D_4) \\ S_6 = \Delta \\ S_7 = \dfrac{1}{2\sqrt{2}}(\psi_1 + \psi_2 + \psi_3 + \psi_4 - \delta_1 - \delta_2 - \delta_3 - \delta_4) \end{cases}$$

$$A_2 \quad S_8 = {}^1/_2(\beta_1 + \beta_2 + \beta_3 + \beta_4)$$

$$B_1\begin{cases} S_9 = {}^1/_2(R_1 - R_2 + R_3 - R_4) \\ S_{10} = {}^1/_2(\gamma_1 - \gamma_2 + \gamma_3 - \gamma_4) \\ S_{11} = {}^1/_2(D_1 - D_2 + D_3 - D_4) \\ S_{12} = \dfrac{1}{2\sqrt{2}}(\psi_1 - \psi_2 + \psi_3 - \psi_4 - \delta_1 + \delta_2 - \delta_3 + \delta_4) \end{cases}$$

$$B_2\begin{cases} S_{13} = {}^1/_2(\beta_1 - \beta_2 + \beta_3 - \beta_4) \\ S_{14} = {}^1/_2(\alpha_{12} - \alpha_{23} + \alpha_{34} - \alpha_{41}) \end{cases}$$

$$E\begin{cases} S_{15} = {}^1/_2(R_1 + R_2 - R_3 - R_4) \\ S_{16} = {}^1/_2(\beta_1 - \beta_2 - \beta_3 + \beta_4) \\ S_{17} = {}^1/_2(\gamma_1 + \gamma_2 - \gamma_3 - \gamma_4) \\ S_{18} = {}^1/_2(D_1 + D_2 - D_3 - D_4) \\ S_{19} = \dfrac{1}{\sqrt{2}}(-\phi_{10,3} - \phi_{10,4}) \\ S_{20} = {}^1/_2(\psi_1 + \psi_2 - \psi_3 - \psi_4) \\ S_{21} = \dfrac{1}{\sqrt{2}}(\alpha_{12} - \alpha_{34}) \\ S_{22} = {}^1/_2(\delta_1 + \delta_2 - \delta_3 - \delta_4) \end{cases}$$

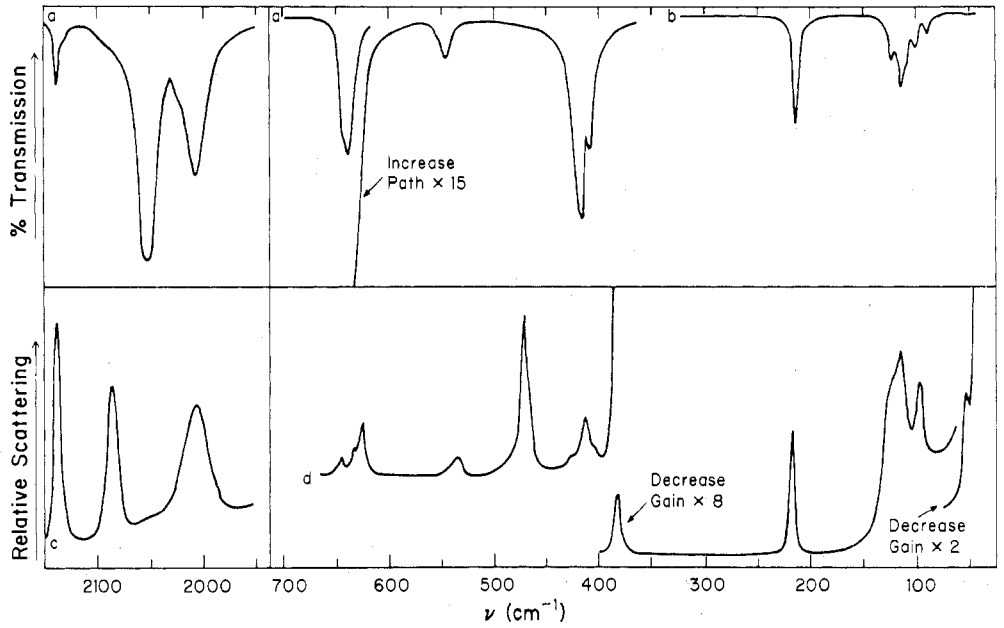

Figure 1. The vibrational spectrum of $Mn(^{12}C^{16}O)_5Br$. The infrared spectrum is presented (a) for CH_2Cl_2 solutions and (b) for a Nujol mull. The Raman spectrum is presented (c) for a CH_2Cl_2 solution and (d) for the solid state as a powder.

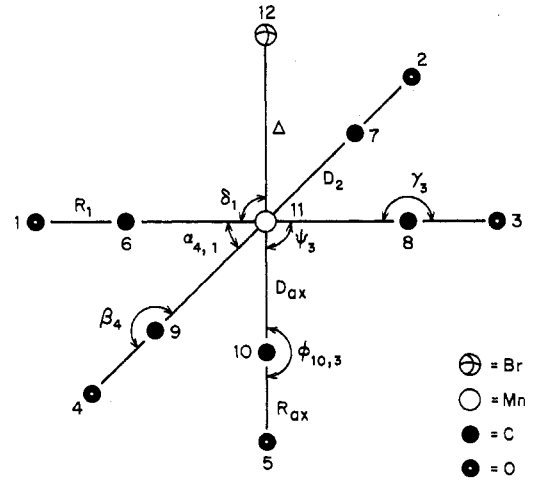

Figure 2. The internal valence coordinates and numbering of atoms for $Mn(CO)_5Br$.

of $Mn(CO)_5Br$, 2 A_1 + B_1 + E, has been assigned a number of times[3,8,14,15] and the same assignment has been adopted here with the refinements of the isotopic data and anharmonicity corrections.

The Region 700–300 cm^{-1}. From previous investigations of metal carbonyl complexes[16] it is expected that the MCO bending and MC stretching modes will lie in this region. It has also been noted that the relative isotopic shifts for ^{13}CO and $C^{18}O$ are quite different for these two types of motion.[2] It was found that for the MCO bending modes only a slight downward shift is noted for the $C^{18}O$ substitution while the ^{13}CO species shows a much greater shift. Conversely, for the MC stretches the $C^{18}O$ species shows a greater downward shift than the ^{13}CO species. This observation leads to the assignment of the observed frequencies from 700 to 500 cm^{-1} as MCO bends and from 500 to 300 cm^{-1} as MC stretches with only one exception as discussed below.

The assignment of the MCO bending modes, $A_1 + A_2 + B_1 + B_2 + 3$ E, is made by consideration of the symmetry correlation between the C_{4v} $Mn(CO)_5Br$ and the O_h $Cr(CO)_6$, as shown in Figure 3. Using the assignments of Jones, *et al.*,[2] for $Cr(CO)_6$ we assign the Raman and unresolved infrared band at 645 cm^{-1} as $A_1(\gamma)$, ν_3, and the strong infrared band at 638 cm^{-1} as the in-plane $E(\beta)$, ν_{16}, mode.

(14) F. A. Cotton, A. Musco, and G. Yagupsky, *Inorg. Chem.*, 6, 1357 (1967).

(15) M. A. El-Sayed and H. D. Kaesz, *J. Mol. Spectrosc.*, 9, 310 (1962).

(16) (a) L. H. Jones, R. S. MacDowell, and M. Goldblatt, *J. Chem. Phys.*, 48, 2663 (1968); (b) D. M. Adams, *J. Chem. Soc.*, 1771 (1964).

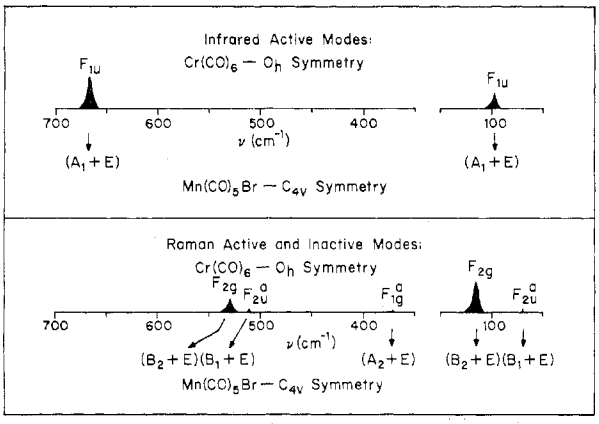

Figure 3. The symmetry correlation between $Cr(CO)_6$ and $Mn(CO)_5Br$ for MCO and CMC bending modes. Superscript a indicates inactive modes for $Cr(CO)_6$; their positions were estimated from the observed combination spectrum.

The frequencies of the unresolved bands were determined by gaussian analysis for all isotopic species.

Both $B_1(\gamma)$ and $B_2(\beta)$ modes should be Raman active only and are attributed to moderate Raman bands at 627 and 537 cm^{-1} (the former is in agreement with the assignment of Butler and Spendjian[17]). The correlation diagram, however, suggests that both modes should be in the vicinity of 530 cm^{-1}. The out-of-plane motion in $B_1(\gamma)$ should result in a greater distortion of the $d\pi$ orbitals of e symmetry than will the in-plane $B_2(\beta)$ mode; this results in the prediction of a larger restoring force for $B_1(\gamma)$ than for $B_2(\beta)$ which is consistent with the assignment of $B_1(\gamma)$ to 627 cm^{-1} and $B_2(\beta)$ to 537 cm^{-1}.

There are then two remaining bands observed in the infrared spectrum which exhibit MCO bending isotopic behavior and may be assigned to the out-of-plane bend, $E(\gamma)$, and the axial bend, $E(\phi)$. The shoulder at 409 cm^{-1} exhibits MCO bending isotopic behavior which eliminates the assignment of Butler and Spendjian[17] of this frequency as the A_1 axial MC stretch. It was also observed that the intensity of this band decreased with increasing distance from the strong E mode at 417 cm^{-1}; this phenomenon, which is illustrated in Figure 4, may be a consequence of a varying degree of interaction between the two fundamentals of E symmetry. The remaining band at 546 cm^{-1} is quite weak. It is not very reasonable to distinguish between differences in $d\pi \rightarrow \pi^*(CO)$ bonding in the b_2 and e orbitals for the $E(\gamma)$ and $E(\phi)$ modes since in these cases the same ligands are not involved in each mode; the matter is further complicated in that $E(\gamma)$ and $E(\phi)$ should be highly mixed in the actual normal modes. Both assignments were tried in the potential constant calculations and will be discussed later.

Except for the band at 409 cm^{-1} already discussed, all observed bands from 500 to 300 cm^{-1} exhibit isotopic behavior characteristic of MC stretching. There are four MC stretching modes expected, $2A_1 + B_1 + E$, of which the two A_1 modes should be polarized in Raman solution spectra. We have found the bands at 381 and 470 cm^{-1} to be polarized. Hyams and Lippincott also observed[18] the 381-cm^{-1} band to be polarized, and Adams and Squire reported[19] that both bands are polarized in agreement with our findings.

(17) I. S. Butler and H. K. Spendjian, *Can. J. Chem.*, **47**, 4117 (1969).
(18) I. J. Hyams and E. R. Lippincott, *Spectrochim. Acta, Part A*, 25, 1845 (1969).
(19) D. M. Adams and A. Squire, *J. Chem. Soc. A*, 2817 (1968).

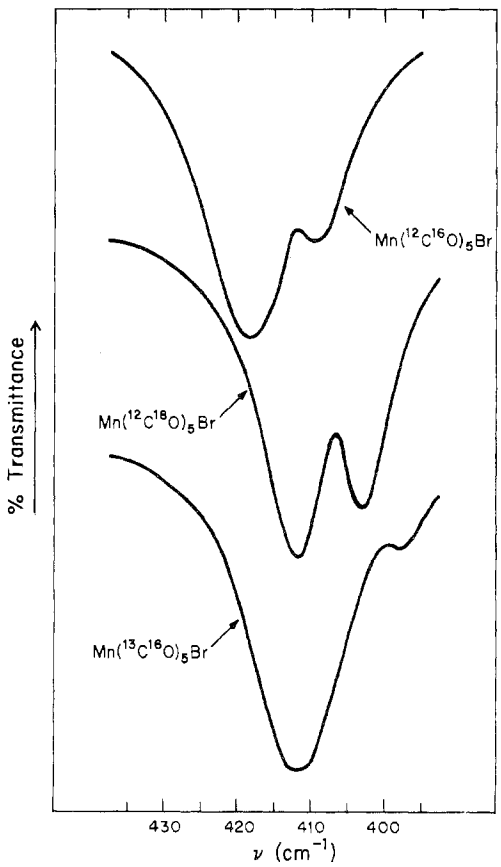

Figure 4. The infrared spectra of three isotopic species in CH_2Cl_2 solution near 400 cm^{-1}. The changes in the relative intensities of the two bands indicate that they are interacting and thus possess the same symmetry, while the changes in energy separation between the two bands on isotopic substitution show that the mode at higher energy is primarily MC stretching, the other mode being MCO bending.

The axial $d\pi(e) \rightarrow \pi^*(CO)$ interaction should be stronger than that in the equatorial $d\pi$ (b_2) level; thus we assign $A_1(D_{ax})$ to 470 cm^{-1} and $A_1(D_{eq})$ to 381 cm^{-1} in agreement with the assignments of Adams and Squire.[19] This argument is supported by the fact that the 470-cm^{-1} band was observed weakly in the infrared spectrum, in contrast to the absence of any infrared absorption corresponding to the 381-cm^{-1} Raman band. These intensity relationships are in agreement with the prediction that the equatorial mode should develop nearly zero change in dipole moment.

The intense infrared band at 417 cm^{-1} is assigned to $E(D_{eq})$. Using the spectral assignments for $Cr(CO)_6$[2] and correlating $A_{1g} \rightarrow A_1$ and $E_g \rightarrow B_1$ we expect the remaining $B_1(D_{eq})$ mode to occur at slightly higher energy than $A_1(D_{eq})$, which is at 381 cm^{-1}. Accordingly we assign $B_1(D_{eq})$ to a moderate peak at 427 cm^{-1} in the solid-state Raman spectrum.

The Region 300-150 cm^{-1}. The metal-bromine stretching mode is of A_1 symmetry and is assigned to the strong Raman polarized band at 222 cm^{-1} in agreement with several previous investigators.[17-21] Isotopic shifts of this frequency are small but definite indicating that it is only slightly mixed with other A_1 modes.

The Region 150-50 cm^{-1}. Our observed frequencies for this region are in excellent agreement with the values reported

(20) R. J. H. Clark and B. C. Crosse, *J. Chem. Soc. A*, 224 (1969).
(21) V. Valenti and F. Cariati, *Inorg. Nucl. Chem. Lett.*, **3**, 237 (1967).

by Hyams and Lippincott.[18] The CMC bending modes, $A_1 + B_1 + B_2 + 2$ E, and the CMBr bending mode, E, are expected in this region, and all the bands observed show the small isotopic shifts characteristic of CMC bends.[2,16a] As bands in solution spectra were extremely weak, it was necessary to make all assignments from solid-state spectra. All bands were accounted for by these bending modes and we do not feel that recourse to assignment of lattice modes above 50 cm^{-1} is necessary for this highly covalent compound. It is essential, however, to postulate site splitting to explain the large number of closely spaced bands observed.

The positions of the CMC bending F_{1u} band of $Cr(CO)_6$[2] and A_1 band of $Mn_2(CO)_{10}$[22] are 103 and 113 cm^{-1}, respectively. These modes correlate with the $A_1(\psi)$ CMC bend for $Mn(CO)_5Br$ and thus it seems reasonable to assign $A_1(\psi)$ to the intense Raman band at 116 cm^{-1}; this mode was observed in the infrared spectrum at 115 cm^{-1}. The medium infrared band at 133 cm^{-1} has no coincident Raman frequency and is assigned with the infrared peak at 122 cm^{-1} as a split E mode. An average value of 127 cm^{-1} was taken for this mode in the potential constant calculations. Similarly the infrared bands at 102 and 87 cm^{-1} are taken to be components of another mode of E symmetry, and the band at 52 cm^{-1} in both Raman and infrared spectra is then the final E mode.

Due to the relatively large mass of Br and the small bond strength of Mn-Br in relation to Mn-CO, it is reasonable to expect that the lowest energy E mode will correspond to CMnBr bending. Thus we assign $E(\delta)$ to the band at 52 cm^{-1}, in agreement with Butler and Spendjian.[17] No clear corroboration of this assignment could be obtained by changing the halogen atom to Cl or I as the spectra of these compounds in the region in question were markedly different from the spectrum of $Mn(CO)_5Br$.[17,18,21] The spectral differences suggest a large amount of mixing among the three internal coordinates of E symmetry, and this was indeed found to be the case in the potential constant calculations below. Both assignments of $E(\psi)$ and $E(\alpha)$ to the frequencies of 127 and 94 cm^{-1} were made in the calculations, and these results are discussed below.

The remaining $B_1(\psi)$ and $B_2(\alpha)$ CMC bending modes were assigned to the intense Raman bands at 99 and 130 cm^{-1}, respectively, on the basis of their correlation with the F_{2u} and F_{2g} modes of $Cr(CO)_6$[2] (see Figure 3). Correlations of this type are quite valuable in the assignment of complex spectral regions, in particular for the nondegenerate modes which do not mix with each other; that these relations have not been used to any great extent in the assignment of CMC bending modes is evident from the large number of inconsistencies in the assignments of these frequencies by previous investigators.[17-21] With the exception of the A_1 mode we regard the assignments in the 150-50-cm^{-1} region as tentative.

The Regions 2600-2200 cm^{-1} and 1200-650 cm^{-1}. The observed infrared combination spectrum for normal $Mn(CO)_5Br$ powder in a KBr pressed disk at room temperature is presented in Table IVA with the frequency assignments. The fundamental frequencies used in the calculation of the combination spectrum are listed in Table IVB. The weak band at 2445 cm^{-1} could not be fitted within ±10 cm^{-1} by any allowed combination of observed fundamentals; thus a value of 395 cm^{-1} was calculated for the inactive A_2 mode, ν_8. The corresponding mode for $Cr(CO)_6$ (Figure 3) occurs at 368 cm^{-1}.

(22) The latter was determined by the polarized Raman spectrum of $Mn_2(CO)_{10}$ in a CH_2Cl_2 solution in these laboratories by D. K. Ottesen (unpublished results).

Table IVA. Observed Sum Combination Spectrum: Solid $Mn(CO)_5Br$ in KBr Pressed Disk

ν_{obsd}, cm^{-1}	Intens	Assignments	Δ, cm^{-1}
652	m	$\nu_{12} + \nu_{17}$	+6
764	vvw	$2\nu_5, \nu_6 + \nu_{17}, \nu_{16} + \nu_{20}, \nu_3 + \nu_7$	−4, −2, +2, +1
788	m	$\nu_5 + \nu_{19}, 2\nu_8$	−3, −2
798	m	$\nu_5 + \nu_{18}$	−3
813	vw	$2\nu_{19}$	−1
879	w	$\nu_4 + \nu_{19}$	−1
899	m	$\nu_4 + \nu_{18}$	+9
940	m	$\nu_{13} + \nu_{19}$	−4
1036	w, br	$\nu_{10} + \nu_{18}, \nu_{10} + \nu_{19}, \nu_3 + \nu_5$	−5, +5, +5
1055	w	$\nu_{10} + \nu_{11}, \nu_{16} + \nu_{18}, \nu_3 + \nu_{19}$	+4, +3, +1
1077	w	$2\nu_{13}$	+3
1168	w	$\nu_{10} + \nu_{17}, \nu_{13} + \nu_{16}$	−6, −4
1191	vw	$\nu_3 + \nu_{17}$	−3
2419	vvw	$\nu_2 + \nu_{18}$	+10
2430	w	$\nu_5 + \nu_{15}$	−4
2445	vvw	$\nu_8 + \nu_{15}$	0
2468	w	$\nu_2 + \nu_4, \nu_{15} + \nu_{18}$	+3, +1
2488	vw	$\nu_9 + \nu_{19}$	0
2497	w	$\nu_9 + \nu_{18}$	−1
2506	w	$\nu_9 + \nu_{11}$	−2
2545	w	$\nu_1 + \nu_{19}$	+1
2555	w	$\nu_1 + \nu_{18}$	+1
2584	vvw	$\nu_{15} + \nu_{16}$	−1

Table IVB. Observed Frequencies for Solid $Mn(CO)_5Br$ Used to Calculate Ir Combination Spectrum

Γ	Mode	ν_{obsd}, cm^{-1}	Γ	Mode	ν_{obsd}, cm^{-1}
A_1	ν_1	2137	B_1	ν_{12}	99
	ν_2	1992[a]			
	ν_3	647	B_2	ν_{13}	537
	ν_4	473		ν_{14}	130
	ν_5	384			
	ν_6	219		ν_{15}	2050
	ν_7	116		ν_{16}	635
				ν_{17}	547
A_2	ν_8	395[b]	E	ν_{18}	417
				ν_{19}	407
B_1	ν_9	2081[a]		ν_{20}	127[c]
	ν_{10}	627		ν_{21}	94[c]
	ν_{11}	427		ν_{22}	53

[a] Average value calculated from observed splittings in the Raman spectrum of the solid (1994 and 1990 cm^{-1} and 2093 and 2079 cm^{-1}, respectively). [b] Calculated from the observed ir combination spectrum. [c] Average value calculated from observed splittings in the ir spectrum of the solid (133 and 122 cm^{-1} and 102 and 87 cm^{-1}, respectively).

The infrared spectrum of these regions has been reported previously.[17] Within these regions we find six bands not reported by Butler and Spendjian[17] while they identify six bands not observed by us. The two sets of assignments are in disagreement for the most part due to the substantial differences in assignments of the fundamental frequencies.

Calculation of Potential Constants

The compliance constants were calculated using the least-squares program of Ottinger.[23] For CO stretches the harmonic frequencies, ω_i, were used. The observed ν_i were employed for other vibrational frequencies. Wherever possible values were taken from solution spectra.

The potential function used is a general quadratic valence field. The elements of C (the compliance constant matrix) are given in Table V and are defined there with reference to Figure 2. The elements of the force constant matrix, F, were obtained from the relation $F = C^{-1}$. The MC and CO

(23) R. S. Ottinger, Ph.D. Thesis, Oregon State University, 1966.

Table V. Elements of Compliance Constant Matrix

A_1 Block

$$C_{1,1} = C_{R_{eq}} + 2C^c_{R_{eq},R_{eq}} + C^t_{R_{eq},R_{eq}}$$
$$C_{2,2} = C_{R_{ax}}$$
$$C_{3,3} = C_\gamma + 2C^c_{\gamma,\gamma} + C^t_{\gamma,\gamma}$$
$$C_{4,4} = C_{D_{ax}}$$
$$C_{5,5} = C_{D_{eq}} + 2C^c_{D_{eq},D_{eq}} + C^t_{D_{eq}}$$
$$C_{6,6} = C_\Delta$$
$$C_{7,7} = C_\psi + 2C^c_{\psi,\psi} + C^t_{\psi,\psi} - C_{\psi,\delta} - 2C^c_{\psi,\delta} - C^t_{\psi,\delta}$$
$$C_{1,2} = 2C^c_{R_{eq},R_{ax}}$$
$$C_{1,3} = C_{R_{eq},\gamma} + 2C^c_{R_{eq},\gamma} + C^t_{R_{eq},\gamma}$$
$$C_{1,4} = 2C^c_{R_{eq},D_{ax}}$$
$$C_{1,5} = C_{R_{eq},D_{eq}} + 2C^c_{R_{eq},D_{eq}} + C^t_{R_{eq},D_{eq}}$$
$$C_{1,6} = 2C_{R_{eq},\Delta}$$
$$C_{1,7} = \frac{1}{\sqrt{2}}(C_{R_{eq},\psi} + 2C^c_{R_{eq},\psi} + C^t_{R_{eq},\psi} - C_{R_{eq},\delta} - 2C^c_{R_{eq},\delta} - C^t_{R_{eq},\delta})$$
$$C_{2,3} = 2C_{R_{ax},\gamma}$$
$$C_{2,4} = C_{R_{ax},D_{ax}}$$
$$C_{2,5} = C_{1,4}$$
$$C_{2,6} = C_{R_{ax},\Delta}$$
$$C_{2,7} = \sqrt{2}(C_{R_{ax},\psi} - C_{R_{ax},\delta}) = \sqrt{2}(C_{R_{ax},\psi'})$$
$$C_{3,4} = 2C_{\gamma,D_{ax}}$$
$$C_{3,5} = C_{\gamma,D_{eq}} + 2C^c_{\gamma,D_{eq}} + C^t_{\gamma,D_{eq}}$$
$$C_{3,6} = 2C_{\gamma,\Delta}$$
$$C_{3,7} = \frac{1}{\sqrt{2}}(C_{\gamma,\psi} + 2C^c_{\gamma,\psi} + C^t_{\gamma,\psi} - C_{\gamma,\delta} - 2C^c_{\gamma,\delta} - C^t_{\gamma,\delta})$$
$$C_{4,5} = 2C_{D_{ax},D_{eq}}$$
$$C_{4,6} = C_{D_{ax},\Delta}$$
$$C_{4,7} = \sqrt{2}(C_{D_{ax},\psi} - C_{D_{ax},\delta}) = \sqrt{2}(C_{D_{ax},\psi'})$$
$$C_{5,6} = 2C_{D_{eq},\Delta}$$
$$C_{5,7} = \frac{1}{\sqrt{2}}(C_{D_{eq},\psi} + 2C^c_{D_{eq},\psi} + C^t_{D_{eq},\psi} - C_{D_{eq},\delta} - 2C^c_{D_{eq},\delta} - C^t_{D_{eq},\delta})$$
$$C_{6,7} = \sqrt{2}(C_{\Delta,\psi} - C_{\Delta,\delta}) = \sqrt{2}(C_{\Delta,\psi'})$$

A_2 Block

$$C_{8,8} = C_\beta + 2C^c_{\beta,\beta} + C^t_{\beta,\beta}$$

B_1 Block

$$C_{9,9} = C_{R_{eq}} - 2C^c_{R_{eq},R_{eq}} + C^t_{R_{eq},R_{eq}}$$
$$C_{10,10} = C_\gamma - 2C^c_{\gamma,\gamma} + C^t_{\gamma,\gamma}$$
$$C_{11,11} = C_{D_{eq}} - 2C^c_{D_{eq},D_{eq}} + C^t_{D_{eq},D_{eq}}$$
$$C_{12,12} = C_\psi - 2C^c_{\psi,\psi} + C^t_{\psi,\psi} - C_{\psi,\delta} + 2C^c_{\psi,\delta} - C^t_{\psi,\delta}$$
$$C_{9,10} = C_{R_{eq},\gamma} - 2C^c_{R_{eq},\gamma} + C^t_{R_{eq},\gamma}$$
$$C_{9,11} = C_{R_{eq},D_{eq}} - 2C^c_{R_{eq},D_{eq}} + C^t_{R_{eq},D_{eq}}$$
$$C_{9,12} = \frac{1}{\sqrt{2}}(C_{R_{eq},\psi} - 2C^c_{R_{eq},\psi} + C^t_{R_{eq},\psi} - C_{R_{eq},\delta} + 2C^c_{R_{eq},\delta} - C^t_{R_{eq},\delta})$$
$$C_{10,11} = C_{\gamma,D_{eq}} - 2C^c_{\gamma,D_{eq}} + C^t_{\gamma,D_{eq}}$$
$$C_{10,12} = \frac{1}{\sqrt{2}}(C_{\gamma,\psi} - 2C^c_{\gamma,\psi} + C^t_{\gamma,\psi} - C_{\gamma,\delta} + 2C^c_{\gamma,\delta} - C^t_{\gamma,\delta})$$
$$C_{11,12} = \frac{1}{\sqrt{2}}(C_{D_{eq},\psi} - 2C^c_{D_{eq},\psi} + C^t_{D_{eq},\psi} - C_{D_{eq},\delta} + 2C^c_{D_{eq},\delta} - C^t_{D_{eq},\delta})$$

B_2 Block

$$C_{13,13} = C_\beta - 2C^c_{\beta,\beta} + C^t_{\beta,\beta}$$
$$C_{14,14} = C_\alpha - 2C^c_{\alpha,\alpha} + C^t_{\alpha,\alpha}$$
$$C_{13,14} = C_{\alpha,\beta} - 2C^c_{\alpha,\beta} + C^t_{\alpha,\beta}$$

E Block

$$C_{15,15} = C_{R_{eq}} - C^t_{R_{eq},R_{eq}}$$
$$C_{16,16} = C_\beta - C^t_{\beta,\beta}$$
$$C_{17,17} = C_\gamma - C^t_{\gamma,\gamma}$$
$$C_{18,18} = C_{D_{eq}} - C^t_{D_{eq},D_{eq}}$$
$$C_{19,19} = C_\phi$$
$$C_{20,20} = C_\psi - C^t_{\psi,\psi}$$
$$C_{21,21} = C_\alpha - C^t_{\alpha,\alpha}$$
$$C_{22,22} = C_\delta - C^t_{\delta,\delta}$$
$$C_{15,16} = C_{R_{eq},\beta} + 2C^c_{R_{eq},\beta} + C^t_{R_{eq},\beta}$$
$$C_{15,17} = C_{R_{eq},\gamma} - C^t_{R_{eq},\gamma}$$
$$C_{15,18} = C_{R_{eq},D_{eq}} - C^t_{R_{eq},D_{eq}}$$
$$C_{15,19} = \sqrt{2}C_{R_{eq},\phi}$$
$$C_{15,20} = C_{R_{eq},\psi} - C^t_{R_{eq},\psi}$$
$$C_{15,21} = \sqrt{2}(C_{R_{eq},\alpha} - C^t_{R_{eq},\alpha})$$
$$C_{15,22} = C_{R_{eq},\delta} - C^t_{R_{eq},\delta}$$
$$C_{16,17} = C_{\beta,\gamma} - C^t_{\beta,\gamma}$$
$$C_{16,18} = C_{\beta,D_{eq}} + 2C^c_{\beta,D_{eq}} + C^t_{\beta,D_{eq}}$$
$$C_{16,19} = \sqrt{2}C_{\beta,\phi}$$
$$C_{16,20} = 2C_{\beta,\psi}$$
$$C_{16,21} = \sqrt{2}(C_{\alpha,\beta} - C^t_{\alpha,\beta})$$
$$C_{16,22} = 2C_{\beta,\delta}$$
$$C_{17,18} = C_{\gamma,D_{eq}} - C^t_{\gamma,D_{eq}}$$
$$C_{17,19} = \sqrt{2}C_{\gamma,\phi}$$
$$C_{17,20} = C_{\gamma,\psi} - C^t_{\gamma,\psi}$$
$$C_{17,21} = \sqrt{2}(C_{\gamma,\alpha} - C^t_{\gamma,\alpha}) = \sqrt{2}C'_{\gamma,\alpha}$$
$$C_{17,22} = C_{\gamma,\delta} - C^t_{\gamma,\delta}$$
$$C_{18,19} = \sqrt{2}C_{D_{eq},\phi}$$
$$C_{18,20} = C_{D_{eq},\psi} - C^t_{D_{eq},\psi}$$
$$C_{18,21} = \sqrt{2}(C_{D_{eq},\alpha} - C^t_{D_{eq},\alpha})$$
$$C_{18,22} = C_{D_{eq},\delta} - C^t_{D_{eq},\delta}$$
$$C_{19,20} = \sqrt{2}C_{\phi,\psi}$$
$$C_{19,21} = 2C_{\phi,\alpha}$$
$$C_{19,22} = \sqrt{2}C_{\phi,\delta}$$
$$C_{20,21} = \sqrt{2}(C_{\psi,\alpha} - C^t_{\psi,\alpha}) = \sqrt{2}C'_{\psi,\alpha}$$
$$C_{20,22} = C_{\psi,\delta} - C^t_{\psi,\delta}$$
$$C_{21,22} = \sqrt{2}(C_{\alpha,\delta} - C^t_{\alpha,\delta}) = \sqrt{2}C'_{\alpha,\delta}$$

bond distances for the recent crystal structure determination[13] of $Mn(CO)_5Cl$ were not available at the time the G matrix was calculated; the parameters used were those determined for $Mn(CO)_5H$ by La Placa, *et al.*:[24] $MC_{ax} = 1.821$ Å, $MC_{eq} = 1.840$ Å, $CO_{ax} = 1.131$ Å, $CO_{eq} = 1.130$ Å. These distances are in close agreement with those determined for

(24) S. J. La Placa, W. C. Hamilton, J. A. Ibers, and A. Davidson, *Inorg. Chem.*, 8, 1928 (1969).

Table VI.

Potential Constant Calculations for A_1 Symmetry Block[a,b]

$C_{1,1}$ = 0.05532 ± 0.00029 (18.144)
$C_{2,2}$ = 0.06057 ± 0.00024 (16.792)
$C_{3,3}$ = 1.394 ± 0.60 (0.740)
$C_{4,4}$ = 0.437 ± 0.43 (2.622)
$C_{5,5}$ = 0.413 ± 0.017 (2.504)
$C_{6,6}$ = 0.843 ± 0.23 (1.318)
$C_{7,7}$ = 1.784 ± 0.97 (0.663)
$C_{1,2}$ = −0.0016 (0.408)
$C_{1,3}$ = 0 (0)
$C_{1,4}$ = 0.0044 (−0.13)
$C_{1,5}$ = −0.0066 ± 0.0030 (0.260)
$C_{1,6}$ = 0 (0)
$C_{1,7}$ = −0.0107 (0.07)
$C_{2,3}$ = 0.0106 (−0.16)
$C_{2,4}$ = −0.0186 ± 0.0063 (0.758)
$C_{2,5}$ = 0.0044 (−0.18)
$C_{2,6}$ = 0 (0.05)
$C_{2,7}$ = 0.0107 (0.02)
$C_{3,4}$ = 0.0775 ± 0.42 (−0.0970)
$C_{3,5}$ = 0 (0)
$C_{3,6}$ = −0.157 ± 0.68 (0.135)
$C_{3,7}$ = −0.045 ± 0.53 (0.0260)
$C_{4,5}$ = 0 (−0.14)
$C_{4,6}$ = −0.088 ± 0.27 (0.369)
$C_{4,7}$ = −0.233 ± 0.88 (0.396)
$C_{5,6}$ = 0 (−0.08)
$C_{5,7}$ = 0.14 (−0.22)
$C_{6,7}$ = −0.241 ± 0.23 (0.236)

Calculated and Observed Frequencies (cm^{-1})

	$Mn(^{12}C^{16}O)_5Br$			$Mn(^{13}C^{16}O)_5Br$			$Mn(^{12}C^{18}O)_5Br$		
ν_i	ν_{obsd}	ν_{calcd}	Δ	ν_{obsd}	ν_{calcd}	Δ	ν_{obsd}	ν_{calcd}	Δ
ν_1	2158.7	2158.8	−0.1	2108.2	2108.1	0.1	2110.6	2110.6	0
ν_2	2030.8	2031.1	−0.3	1984.2	1984.0	0.2	1985.0	1984.9	0.1
ν_3	645.0	645.9	−0.9	632.0	631.7	0.3	641.3	640.8	0.5
ν_4	470.4	470.5	−0.1	462.2	462.3	0.1	459.8	459.8	0
ν_5	380.5	380.5	0	374.8	374.4	0.4	366.5	366.9	−0.4
ν_6	222.4	222.5	−0.1	221.6	221.5	0.1	220.6	220.6	0
ν_7	115.8	114.8	1.0	114.0	114.4	−0.4	109.9	110.6	−0.7

[a] Error limits for $C_{i,j}$ are calculated standard deviations; those without standard deviations were held constant in the calculation. Units for $C_{i,j}$ are Å mdyn^{-1} for stretch-stretch, radian mdyn^{-1} for stretch-bend, and radian^2 Å^{-1} mdyn^{-1} for bend-bend. [b] Equivalent $F_{i,j}$ are given in parentheses. Units are inverse of corresponding $C_{i,j}$.

Table VII.[a,b]

B_1 Block

Potential Constant Calculation

$C_{9,9}$ = 0.05750 ± 0.00061 (17.770)
$C_{10,10}$ = 0.945 ± 0.003 (1.211)
$C_{11,11}$ = 0.349 ± 0.009 (3.014)
$C_{12,12}$ = 2.150 ± 0.054 (0.547)
$C_{9,10}$ = 0 (0.07)
$C_{9,11}$ = −0.0198 ± 0.0073 (1.06)
$C_{9,12}$ = −0.0053 (0.04)
$C_{10,11}$ = 0 (0.12)
$C_{10,12}$ = −0.5 (0.29)
$C_{11,12}$ = −0.14 (0.23)

Calculated and Observed Frequencies (cm^{-1})

	$Mn(^{12}C^{16}O)_5Br$			$Mn(^{13}C^{16})_5Br$			$Mn(^{12}C^{18}O)_5Br$		
ν_i	ν_{obsd}	ν_{calcd}	Δ	ν_{obsd}	ν_{calcd}	Δ	ν_{obsd}	ν_{calcd}	Δ
ν_9	2083.8	2084.3	−0.5	2036.7	2036.3	0	2036.5	2036.4	0.1
ν_{10}	626.8	630.2	−3.4	613.4	611.3	2.1	623.2	621.9	1.3
ν_{11}	427.1	425.9	1.2	418.5	418.8	−0.3	410.1	411.0	−0.9
ν_{12}	99.0	99.5	−0.5	98.5	98.5	0	95.6	95.0	0.6

B_2 Block

Potential Constant Calculation

$C_{13,13}$ = 1.692 ± 0.032 (0.593)
$C_{14,14}$ = 1.696 ± 0.09 (0.592)
$C_{13,14}$ = −0.1 (0.035)

Calculated and Observed Frequencies (cm^{-1})

	$Mn(^{12}C^{16}O)_5Br$			$Mn(^{13}C^{16}O)_5Br$			$Mn(^{12}C^{18}O)_5Br$		
ν_i	ν_{obsd}	ν_{calcd}	Δ	ν_{obsd}	ν_{calcd}	Δ	ν_{obsd}	ν_{calcd}	Δ
ν_{13}	537.4	537.2	−0.2	517.4	518.6	−1.2	534.7	533.7	+1.0
ν_{14}	129.6	130.4	−0.8	128.6	129.6	−1.0	122.8	123.8	−1.0

[a] Error limits for $C_{i,j}$ are calculated standard deviations; those without standard deviations were held constant in the calculation. Units for $C_{i,j}$ are Å mdyn^{-1} for stretch-stretch, radian mydn^{-1} for stretch- bend, and radian^2 Å^{-1} mdyn^{-1} for bend-bend. [b] Equivalent $F_{i,j}$ are given in parentheses. Units are inverse of corresponding $C_{i,j}$.

$Mn(CO)_5Cl$.[13] The MnBr distance was estimated from Pauling's table of covalent radii[25] to be 2.4 Å.

A_1 Symmetry Compliance Constants. The calculations for the A_1 symmetry block are found in Table VI. The estimated errors, ϵ_i, in the observed frequencies, ν_i, were used to weight these data in the least-squares calculation. Each eigenvalue ($\phi = 1/4\pi^2\nu_i^2$) was weighted[26] as ν_i^6/ϵ_i^2.

Starting values for the $C_{i,j}$ were obtained from the calculations of Jones, *et al.*,[2] for the $M(CO)_6$ systems. It was found that a stable solution for the 7 × 7 matrix could be obtained only by restraining 13 of the total 28 $C_{i,j}$ to their starting values. From examination of the Jacobian (*JZ*) matrix[23] it was determined which $C_{i,j}$ had the least effect on the frequencies and those elements of *C* were then the ones held fixed.

A_2 Symmetry Compliance Constant. From the observed ir combination spectra a frequency of 395 cm^{-1} was calculated for the inactive A_2 mode. From the calculated valence constants of the B_2 and E symmetry blocks, however, a value of 2.275 radian^2 Å^{-1} mdyn^{-1} for $C_{(A_2)}$ was estimated and a frequency of ν_8 = 404.7 cm^{-1} was calculated

(25) L. Pauling, "The Nature of the Chemical Bond," 3rd ed, Cornell University Press, Ithaca, N. Y., 1960.
(26) L. H. Jones, *J. Mol. Spectrosc.*, 34, 108 (1970).

Table VIII.

Potential Constant Calculation for E Symmetry Block[a,b]

$C_{15,15}$ = 0.05743 ± 0.00011 (17.811)
$C_{16,16}$ = 1.483 ± 0.003 (0.731)
$C_{17,17}$ = 2.682 ± 0.011 (0.393)
$C_{18,18}$ = 0.822 ± 0.010 (1.425)
$C_{19,19}$ = 2.691 ± 0.009 (0.452)
$C_{20,20}$ = 1.7[c] (0.764)
$C_{21,21}$ = 2.1[c] (0.673)
$C_{22,22}$ = 5.2[c] (0.291)
$C_{15,16}$ = −0.01 (0.069)
$C_{15,17}$ = 0 (−0.016)
$C_{15,18}$ = −0.0311 ± 0.0081 (0.714)
$C_{15,19}$ = 0.007 (0.106)
$C_{15,20}$ = 0 (0.043)
$C_{15,21}$ = −0.011 (0.067)
$C_{15,22}$ = 0 (0.027)
$C_{16,17}$ = 0 (0.005)
$C_{16,18}$ = −0.16 (−0.055)
$C_{16,19}$ = −0.5[c] (0.119)
$C_{16,20}$ = 0.06 (−0.036)
$C_{16,21}$ = 0.16 (−0.075)
$C_{16,22}$ = 0.06 (−0.032)
$C_{17,18}$ = 0.0489[c] (−0.032)
$C_{17,19}$ = −0.074[c] (−0.003)
$C_{17,20}$ = 0.46 (−0.097)
$C_{17,21}$ = 0 (0.003)
$C_{17,22}$ = −0.46 (0.019)
$C_{18,19}$ = −0.5[c] (0.253)
$C_{18,20}$ = 0 (0.032)
$C_{18,21}$ = 0.14 (−0.086)
$C_{18,22}$ = 0 (−0.014)
$C_{19,20}$ = −0.28 (0.090)
$C_{19,21}$ = −0.06 (0.019)
$C_{19,22}$ = −0.13 (0.031)
$C_{20,21}$ = −0.25[c] (0.225)
$C_{20,22}$ = −0.90[c] (0.189)
$C_{21,22}$ = −1.45[c] (0.228)

Calculated and Observed Frequencies (cm^{-1})

	$Mn(^{12}C^{16}O)_5Br$			$Mn(^{13}C^{16}O)_5Br$			$Mn(^{12}C^{18}O)_5Br$		
ν_i	ν_{obsd}	ν_{calcd}	Δ	ν_{obsd}	ν_{calcd}	Δ	ν_{obsd}	ν_{calcd}	Δ
ν_{15}	2078.5	2079.1	−0.6	2032.8	2032.6	0.2	2029.7	2029.3	0.4
ν_{16}	638.4	638.9	−0.5	622.0	622.6	−0.6	636.2	635.0	1.2
ν_{17}	545.5	545.7	−0.2	527.1	527.0	0.1	524.8	524.6	0.2
ν_{18}	417.2	417.5	−0.3	411.7	412.2	−0.5	411.2	410.3	0.9
ν_{19}	408.5	408.5	0	396.8	395.7	1.1	402.7	403.9	−1.2
ν_{20}	127.0	126.7	0.3		125.9			121.6	
ν_{21}	94.0	93.8	0.2		93.3			89.0	
ν_{22}	52.9	52.4	0.5	52.5	52.1	0.4	51.0	50.9	0.1

[a] Error limits for $C_{i,j}$ are calculated standard deviations; those without standard deviations were held constant in the calculation. Units for $C_{i,j}$ are Å mdyn^{-1} for stretch-stretch, radian mdyn^{-1} for stretch-bend, and radian^2 Å^{-1} mdyn^{-1} for bend-bend. [b] Equivalent $F_{i,j}$ are given in parentheses. Units are inverse of corresponding $C_{i,j}$. [c] $C_{i,j}$ adjusted manually for best fit of observed frequencies.

for the normal species. This rather close agreement of values from two sources is highly encouraging for the accuracy of our frequency assignments and potential constant solution in view of the large uncertainties regarding the 150-50-cm^{-1} region of the spectrum.

B_1 Symmetry Compliance Constants. This calculation is shown in Table VII. It was necessary to hold constant five elements of C to obtain convergence. The fit of ν_{10} (the MCO bending mode) was rather poor, the accuracy being only ±2.7 cm^{-1} for the three isotopic species. Careful manipulation of $C_{10,11}$ and $C_{10,12}$ or assignment of this frequency as a B_2 mode did not improve the fit. As this band was observed with a precision of ±0.2 cm^{-1}, the poor fit may be due to the different interactions of each isotopic species with nearby modes of the same symmetry in the solid state. These interactions arise from the lowering of the molecular symmetry C_{4v} in solution to site symmetry C_s in the solid state.[13]

B_2 Symmetry Compliance Constants. Rapid convergence for this 2 × 2 block of bending modes was obtained for the calculation shown in Table VII.

E Symmetry Compliance Constants. This was by far the most complex calculation undertaken and the best results are presented in Table VIII. The amount of mixing between the two CMC bending and CMBr bending modes is very large as was predicted on the basis of comparisons among the spectra of $Mn(CO)_5Cl$, $Mn(CO)_5Br$, and $Mn(CO)_5I$. This made it necessary to constrain all $C_{i,j}$ having to do exclusively with CMC or CMBr bending modes. The primary constants, $(C_\alpha)_E$, $(C_\psi)_E$, and $(C_\delta)_E$, and the most significant interaction constants were adjusted manually for the best fit. The number of $C_{i,j}$ which could be varied was further limited by the strong mixing of the three MCO internal bending coordinates.

Calculations were tried for the assignments of $E(\gamma)$ to 408 cm^{-1} and $E(\phi)$ to 546 cm^{-1}, and *vice versa*. The second calculation showed very little mixing between the out-of-plane equatorial MCO bend, γ, and the axial MCO bend, ϕ, while ϕ was found to be considerably mixed with the in-plane equatorial MCO bend, β. This is not as kinetically reasonable as the first calculation which showed γ and ϕ to be highly mixed with each other and with relatively little mixing of either with β. Furthermore it was found that the valence constants C_γ, $C^c_{\gamma,\gamma}$, and $C^t_{\gamma,\gamma}$ agree far better with the analogous quantities for $Cr(CO)_6$ in the first calculation than in the second. For these reasons we adopt the assignments $E(\gamma) \rightarrow 408$ cm^{-1} and $E(\phi) \rightarrow 546$ cm^{-1} and present the corresponding potential constant calculation in Table VIII.

As was the case for the hexacarbonyl systems, the in-plane MCO and in-plane CMC bending modes are strongly coupled (this constant was quite significant and was allowed to vary). The most reasonable values for the potential constants (from the viewpoint of transferability) were obtained when $E(\psi)$ was assigned to the infrared bands centered at 94 cm^{-1}. From the resulting potential energy distribution (Table IX) it was found that $E(\alpha)$ is fairly well distributed among all three low-energy modes of E symmetry.

Characterization of the Normal Vibrations. We report in Table IX the potential energy, V_{kl,v_i}, as arising from a particular internal coordinate, L_{k,v_i}, for $Mn(^{12}C^{16}O)_5Br$. These values were obtained from the relation $V_{kl,v_i} = L_{k,v_i}(C^{-1})_{kl} \cdot L_{l,v_i}$ and they resemble closely the values reported[2] for $M(CO)_6$ when comparing the A_1, B_1, and B_2 blocks with the analogous coordinates of the $A_{1g} + F_{1u}$, $E_g + F_{2u}$, and $E_g + F_{2g}$ blocks, respectively. The various coordinates found in the E block for $Mn(CO)_5Br$ in most cases do not mix in the $M(CO)_6$ systems, and thus the distributions of V_{kl,v_i} for this block cannot be readily compared to the analogous coordinates for the more symmetrical hexacarbonyls. As was found earlier,[2,11,16,27] there is a large amount of mixing in the normal modes of the MC and CO

(27) (a) L. H. Jones, *J. Chem. Phys.*, 36, 2375 (1962); (b) H. Murata and K. Kuwai, *Bull. Chem. Soc. Jap.*, 33, 1008 (1960); (c) I. J. Hyams, D. Jones, and E. R. Lippincott, *J. Chem. Soc. A*, 1987 (1967).

Table IX. Potential Energy Distribution

A_1 Symmetry Block

	ν_1	ν_2	ν_3	ν_4	ν_5	ν_6	ν_7
$C_{1,1}$	0.90	0.07			0.03		
$C_{2,2}$	0.06	0.94	0.01	0.01			
$C_{3,3}$			0.60	0.22	0.01		0.20
$C_{4,4}$		0.05	0.15	0.70	0.02	0.03	0.19
$C_{5,5}$	0.04				0.96		0.02
$C_{6,6}$			0.03	0.04		0.99	0.06
$C_{7,7}$			0.21			0.15	0.83
$C_{1,2}$	0.01	−0.01					
$C_{1,3}$							
$C_{1,4}$							
$C_{1,5}$					0.01		
$C_{1,6}$							
$C_{1,7}$							
$C_{2,3}$			−0.01				
$C_{2,4}$		−0.05	0.01	0.01			
$C_{2,5}$							
$C_{2,6}$							
$C_{2,7}$							
$C_{3,4}$			−0.04	0.06			−0.03
$C_{3,5}$							
$C_{3,6}$			−0.03	0.03			−0.03
$C_{3,7}$			0.03				−0.03
$C_{4,5}$				0.01	−0.02		0.01
$C_{4,6}$			−0.02	−0.06		0.07	−0.04
$C_{4,7}$			0.11	−0.02		−0.04	−0.24
$C_{5,6}$							
$C_{5,7}$			0.01		−0.02		−0.05
$C_{6,7}$			−0.04			−0.19	0.11

B Symmetry Blocks

	B_1				B_2		
	ν_9	ν_{10}	ν_{11}	ν_{12}		ν_{13}	ν_{14}
$C_{9,9}$	1.01		0.01		$C_{13,13}$	0.75	0.25
$C_{10,10}$		1.14		0.01	$C_{14,14}$	0.31	0.70
$C_{11,11}$	0.06		0.96	0.03	$C_{13,14}$	−0.05	0.05
$C_{12,12}$		0.09		1.09			
$C_{9,10}$							
$C_{9,11}$	−0.07		0.03				
$C_{9,12}$							
$C_{10,11}$							
$C_{10,12}$		−0.23		−0.06			
$C_{11,12}$			0.01	−0.07			

E Symmetry Block

	ν_{15}	ν_{16}	ν_{17}	ν_{18}	ν_{20}	ν_{20}	ν_{21}	ν_{22}
$C_{15,15}$	1.02							
$C_{16,16}$		0.63		0.14		0.30	0.01	0.01
$C_{17,17}$			0.11		0.66		0.22	0.05
$C_{18,18}$	0.03	0.08		0.79		0.28		
$C_{19,19}$			0.42		0.24	0.38	0.17	0.01
$C_{20,20}$		0.01	0.31	0.02		0.04	0.88	0.03
$C_{21,21}$		0.18				0.33	0.27	0.64
$C_{22,22}$			0.01	0.01	0.05	0.05	0.06	1.34
$C_{15,16}$								
$C_{15,17}$								
$C_{15,18}$	−0.05			0.01		−0.01		
$C_{15,19}$								
$C_{15,20}$								
$C_{15,21}$								
$C_{15,22}$								
$C_{16,17}$								
$C_{16,18}$		−0.02		0.04		−0.03		
$C_{16,19}$		−0.01	0.02	0.01	−0.01	−0.13	0.02	
$C_{16,20}$						−0.01	0.01	
$C_{16,21}$		0.07				−0.07	−0.01	−0.02
$C_{16,22}$				−0.01		−0.02		0.02
$C_{17,18}$								
$C_{17,19}$								
$C_{17,20}$			0.07		0.02		−0.16	−0.01
$C_{17,21}$								
$C_{17,22}$					0.02		−0.01	−0.03
$C_{18,19}$		−0.01	−0.01	−0.02		−0.20	−0.02	
$C_{18,20}$					0.02		−0.01	
$C_{18,21}$		0.02				−0.05	0.01	
$C_{18,22}$						−0.01		
$C_{19,20}$			0.11		−0.01	−0.04	−0.12	
$C_{19,21}$						−0.02	0.02	
$C_{19,22}$			0.01		0.02	−0.02	0.02	−0.01
$C_{20,21}$		0.03				0.07	−0.30	0.08
$C_{20,22}$			−0.03	0.01	−0.01	0.04	−0.19	−0.16
$C_{21,22}$		0.02			0.01	0.13	0.13	−0.95

stretching coordinates and also of the MCO and CMC bending coordinates. This mixing is in part due to the starting values chosen for the $C_{i,j}$ and the constraints placed upon them.

Valence Potential Constants. The values of stretch-stretch and bend-bend potential constants are listed in Table X and are calculated from the symmetry potential constants given in Tables VI-VIII and the relations in Table V. Values for stretch-bend interactions have been with few exceptions held equal to the analogous quantities for $M(CO)_6$. Those which were allowed to be refined in the least-squares program were found to be rather poorly determined in most cases (which was also found previously[2]).

Discussion

Primary Stretching Potential Constants. From Table X we compare $C_{R_{eq}}$ and $C_{R_{ax}}$ to C^*_{CO} and $C_{D_{eq}}$ and $C_{D_{ax}}$ to C^*_{MC} (in the following discussion we will indicate all compliance and force constants for the $M(CO)_6$ systems with an asterisk). In the first case we have $C_{R_{eq}} < C^*_{CO}$ while $C_{R_{ax}} \approx C^*_{CO}$; this implies a smaller total amount of $d\pi(MC) \rightarrow \pi^*(CO)$ bonding in $Mn(CO)_5Br$ as compared to the hexacarbonyls, while the effect of ligand substitution is to decrease preferentially the axial CO π-bond strength as noted previously.[3,8] The overall effect must be due to the larger energy difference between the metal $d\pi$ orbitals and the $\pi^*(CO)$ orbitals caused by the higher positive charge on the central metal atom in the case of $Mn(CO)_5Br$.

We also note that $C_{D_{eq}} > C^*_{MC}$ where the large value for $C_{D_{eq}}$ supports the hypothesis of an overall decrease in $d\pi(MC) \rightarrow \pi^*(CO)$ bonding. On the other hand axial $d\pi(MC) \rightarrow \pi^*(CO)$ bonding should not be decreased as much compared to the equatorial MC system,[8,28] and a simultaneous increase in total MC σ bonding is sufficient to explain the observed relation $C_{D_{ax}} < C^*_{MC}$. Analogous changes in M-CO σ and π bonding on increasing the positive charge of the metal atom have been suggested previously for the series $V(CO)_6^-$, $Cr(CO)_6$, $Mn(CO)_6^+$; and $W(CO)_6$, $Re(CO)_6^+$.[29-31]

We have observed a Raman frequency of 188 cm^{-1} for the Cr-Br stretching mode of $[N(C_2H_5)_4][Cr(CO)_5Br]$. Clark

(28) R. F. Fenske and R. L. DeKock, *Inorg. Chem.*, 9, 1053 (1970).

(29) E. W. Abel, R. A. N. McLean, S. P. Tyfield, P. S. Braterman, A. P. Walter, and P. J. Hendra, *J. Mol. Spectrosc.*, 30, 29 (1969).

(30) K. G. Caulton and R. F. Fenske, *Inorg. Chem.*, 7, 1273 (1968).

(31) N. A. Beach and H. B. Gray, *J. Amer. Chem. Soc.*, 90, 5713 (1968).

Table X. Internal Coordinate Valence Potential Constants

$C_{i,j}$	Calcd for $Mn(CO)_5Br$ Compl const, Å mdyn^{-1}	Force const, mdyn Å^{-1}	Approx equiv for $M(CO)_6$	Calcd for $M(CO)_6$ Compl const, Å mdyn^{-1}	Force const, mdyn Å^{-1}
		Stretch–Stretch Constants			
$C_{R_{eq}}$	0.05692	17.884	C_{CO}	0.05905[b]	17.04[b]
$C_{R_{ax}}$	0.06057	16.792	C_{CO}	0.05905[b]	17.04[b]
$C_{D_{eq}}$	0.602	2.092	C_{MC}	0.509[b]	2.10[b]
$C_{D_{ax}}$	0.437	2.622	C_{MC}	0.509[b]	2.10[b]
C_{Δ}	0.843	1.318			
$C^{c}_{R_{eq}, R_{eq}}$	−0.00051	0.094	$C^{c}_{CO, C'O'}$	−0.00077	0.175
$C^{t}_{R_{eq}, R_{eq}}$	−0.00055	0.073	$C^{t}_{CO, C'O'}$	−0.00025	0.039
$C^{c}_{R_{eq}, R_{ax}}$	−0.0008[a]	0.204	$C^{c}_{CO, C'O'}$	−0.00077	0.175
$C^{c}_{D_{eq}, D_{eq}}$	0.016	−0.128	$C^{c}_{MC, MC'}$	0.0023[b]	−0.02[b]
$C^{t}_{D_{eq}, D_{eq}}$	−0.220	0.667	$C^{t}_{MC, MC'}$	−0.114[b]	0.47[b]
$C^{c}_{D_{eq}, D_{ax}}$	0[a]	−0.07	$C^{c}_{MC, MC'}$	0.0023[b]	−0.02[b]
$C_{R_{eq}, D_{eq}}$	−0.0222	0.688	$C_{CO, MC}$	−0.0238	0.758
$C^{c}_{R_{eq}, D_{eq}}$	0.0033	−0.200	$C^{c}_{CO, MC'}$	0.0022	−0.088
$C^{t}_{R_{eq}, D_{eq}}$	0.0089	−0.26	$C^{t}_{CO, MC'}$	0.0097	−0.112
$C^{c}_{R_{eq}, D_{ax}}$	0.0022[a]	−0.065	$C^{c}_{CO, MC'}$	0.0022	−0.888
$C^{c}_{R_{ax}, D_{eq}} \equiv C^{c}_{R_{eq}, D_{ax}}$					
$C_{R_{ax}, D_{ax}}$	−0.0186	0.758	$C_{CO, MC}$	−0.0238	0.758
$C_{R_{eq}, \Delta}$	0[a]	0			
$C_{R_{ax}, \Delta}$	0[a]	0			
$C_{D_{eq}, \Delta}$	0[a]	−0.04			
$C_{D_{ax}, \Delta}$	−0.088	0.363			
		Bend–Bend Constants			
C_{β}	1.733	0.663	C_{β}	1.919	0.48
C_{γ}	1.901	0.685	C_{β}	1.919	0.48
C_{ϕ}	2.691	0.452	C_{β}	1.919	0.48
$C_{\psi} - C_{\psi, \delta}$	2.147	0.615	$C_{\alpha} - C''''_{\alpha}$	2.62	0.56
$C_{\psi} - C^{t}_{\psi, \psi}$	1.7	0.76	$C_{\alpha} - C''''_{\alpha}$	2.62	0.56
$C_{\delta} - C^{t}_{\delta, \delta}$	5.2	0.29			
C_{α}	2.12	0.632	C_{α}	1.92	0.518
$C^{c}_{\beta, \beta}$	0.146	0.001	$-C''_{\beta, \beta}$	0.07	−0.023
$C^{t}_{\beta, \beta}$	0.25[a]	−0.068	$-C'_{\beta, \beta}$	0.25	−0.068
$C^{c}_{\gamma, \gamma}$	0.112	−0.118	$C'''_{\beta, \beta}$	0.24	−0.029
$C^{t}_{\gamma, \gamma}$	−0.781	0.292	$C'_{\beta, \beta}$	−0.25	0.068
$C^{t}_{\psi, \psi} - C^{t}_{\psi, \delta}$	−0.18[a]	0.01	$C''''_{\alpha, \alpha} - C''_{\alpha, \alpha}$	−0.18	0.01
$C^{c}_{\psi, \psi} - C^{c}_{\psi, \delta}$	−0.093	0.03	$C'_{\alpha, \alpha} - C'''_{\alpha, \alpha}$	−0.44	0.13
$C^{c}_{\alpha, \alpha}$	0.22[a]		$C''''_{\alpha, \alpha}$	0.22	
$C^{t}_{\alpha, \alpha}$	0.02		$C''_{\alpha, \alpha}$	−0.52	
$C_{\beta, \gamma} = C^{c}_{\beta, \gamma} = C^{t}_{\beta, \gamma} \equiv 0$					
$C_{\beta, \phi}$	−0.18	0.042	$-C'''_{\beta, \beta}$	−0.25	0.029
$C_{\gamma, \phi} - C^{t}_{\gamma, \phi}$	−0.05	−0.0023	$C''_{\beta, \beta}$	−0.07	0.023
$C_{\psi, \delta} - C^{t}_{\psi, \delta}$	−0.9	0.189	$C''''_{\alpha, \alpha} - C''_{\alpha, \alpha}$	−0.18	0.01
$C'_{\psi, \alpha}$	−0.09	0.08	$C'_{\alpha, \alpha}$	−0.22	0.14
$C'_{\delta, \alpha}$	−0.51	0.08	$C'_{\alpha, \alpha}$	−0.22	0.14
$C_{\beta, \psi}$	0.03[a]	−0.018	$C'''_{\alpha, \beta}$	0.03	−0.015
$C_{\beta, \delta}$	0.03[a]	−0.010	$C'''_{\alpha, \beta}$	0.03	−0.015
$C_{\beta, \alpha}$	0.03	−0.02	$C'_{\alpha, \beta}$	0.51	−0.11
$C^{c}_{\beta, \alpha}$	−0.07	0.038	$-C''_{\alpha, \beta}$	−0.09	0.04
$C_{\gamma, \psi'} + C^{t}_{\gamma, \psi'}$	−0.20	0.22	$-C'_{\alpha, \beta} - C''_{\alpha, \beta}$	−0.64	0.152
$C^{c}_{\gamma, \psi'}$	0.08	−0.001	$C'''_{\alpha, \beta}$	0.03	−0.015
$C_{\gamma, \psi} - C^{t}_{\gamma, \psi}$	0.46[a]	−0.097	$C_{\alpha, \beta} - C''_{\alpha, \beta}$	0.46	−0.068
$C_{\gamma, \delta} - C^{t}_{\gamma, \delta}$	−0.46[a]	0.019	$-C_{\alpha, \beta} + C''_{\alpha, \beta}$	−0.46	0.068
$C'_{\gamma, \alpha}$	0[a]				
$C_{\phi, \psi}$	−0.20	0.064	$-C'_{\alpha, \beta}$	−0.51	0.11
$C_{\phi, \delta}$	−0.09[a]	0.022	$-C''_{\alpha, \beta}$	−0.09	0.042
$C_{\phi, \alpha}$	−0.03[a]	0.013	$-C'''_{\alpha, \beta}$	−0.03	0.015

[a] Denotes values held constant (*i.e.*, transferred directly from the $M(CO)_6$ system) for $C_{i,j}$ in calculation. [b] Where the value of $C_{i,j}$ for $Cr(CO)_6$ differs significantly from average of $Cr(CO)_6$, $Mo(CO)_6$, and $W(CO)_6$, the value for $Cr(CO)_6$ was used.

and Crosse[20] have reported a Raman frequency of 175 cm^{-1} for this anion.

From our observation we have estimated a value of 0.995 Å $mdyn^{-1}$ for C_Δ which is a significant increase in compliance from the value of $C_\Delta = 0.843$ Å $mdyn^{-1}$ for $Mn(CO)_5Br$. This comparison indicates the strengthening of the M-Br σ-bonding system in $Mn(CO)_5Br$ relative to $Cr(CO)_5Br^-$.

Stretch-Stretch Interaction Constants. These constants are found in Table X. It is of great interest to compare CO,C′ O′ stretching interaction force constants of the present normal-coordinate analysis with the results of previous simplified, "CO energy factored," anharmonic approximations.[3,8,14] In contrast to the assumed relation $k^t_{CO,C'O'} \approx 2k^c_{CO,C'O'}$,[14] we find $F^t_{CO,C'O'} \approx {}^3/_4 F^c_{CO,C'O'}$. Thus, as with $M(CO)_6$,[2] we find that the exclusive π-bonding interaction model does not explain the experimental observations.[2,29] The large value of the cis constant relative to the trans constant is in agreement with the electrostatic model of Haas and Sheline[32] and Jones, *et al.*,[2] who proposed that CO,C′O′ interactions arise as a result of mutual polarizations caused by the large oscillating CO dipole moments.

We find the MC,CO and MC,C′O′ interactions to be quite similar to the values for $M(CO)_6$. $C_{R_{ax},D_{ax}}$ and $C_{R_{eq},D_{eq}}$ are large coupling constants and are approximately equal; from these observations and the considerable differences among the various MC and CO bond strengths, the significant σ-bonding and π-bonding changes must counterbalance to account for the observed interactions.

The most significant interaction of the Mn-Br stretching coordinate, Δ, is with the axial MC coordinate, D_{ax} ($C_{\Delta,D_{ax}} = 0.088$ Å $mdyn^{-1}$ and $F_{\Delta,D_{ax}} = 0.363$ mdyn $Å^{-1}$). Fenske and DeKock[28] have noted in their molecular orbital calculations for $Mn(CO)_5X$ systems that there is no net π-electron donation from the halogen to the metal atom. Thus, when Δ is increased and the Mn-Br bond is weakened, the positive charge on the Mn atom becomes larger which in turn increases the total MC σ-bond order, while decreasing the total MC π-bond order. If it is assumed that all MC σ-bond strengths will increase in the same proportion, then the axial MC π bonding will be diminished less than will the weaker equatorial MC π bonds by the increasing positive charge on the metal atom. This model explains the observed relation $C_{\Delta,D_{ax}} < 0$ while $C_{\Delta,D_{eq}} = 0$ and is quite similar to the analysis of the MC stretching constants, $C_{D_{ax}}$ and $C_{D_{eq}}$.

Bending Potential Constants. These values are found in Table X. The greatest difference in bending constants between $Mn(CO)_5Br$ and $M(CO)_6$ was found in the axial MCO bend, C_ϕ, which is considerably larger than C_β, C_γ, or C_β*. This greater compliance is contradictory to the prevalent concept of increased axial MC π bonding which would lead to a less compliant axial MCO bend in $M(CO)_5L$ complexes where L is not a π-electron acceptor. The unexpectedly large value for C_ϕ is probably due to uncertainties in our vibrational analysis, as the only relations defining this constant are from the rather poorly determined E symmetry block calculation. Small changes in the frequency assignments of the CMC bending vibrations and in the bend-bend interaction constants of the E block would suffice to alter the present relations among the primary MCO bending constants (C_β, C_γ, and C_ϕ) with only a small deterioration, if any, in the frequency fit. Thus, for the present calculation we have established only that the *overall* values of compliance constants for MCO bending in $Mn(CO)_5Br$ are larger than C_β* for $M(CO)_6$, which is consistent with the smaller amount of MC π bonding expected for the Mn(I) complex as compared with $Cr(CO)_6$.

Except for the CMC bend, $A_1(\psi)$, we regard the assignments for the spectral region below 200 cm^{-1} as tentative, and we do not attach much significance to their respective potential constants.

Stretch-bend interactions are quite complex and were found to be rather poorly determined in the calculations.[33,34] Furthermore, most of their values are not significantly different from zero so that a more detailed discussion of them is not meaningful at this time.

Registry No. $Mn(^{12}C^{16}O)_5Br$, 14516-54-2; $Mn(^{13}C^{16}O)_5Br$, 16457-28-6; $Mn(^{12}C^{18}O)_5Br$, 19217-82-4.

Acknowledgments. We are grateful to R. M. Potter of Los Alamos for supplying us with the $^{15}N^{18}O$. This work was supported by the California Institute of Technology, the National Science Foundation, and the U. S. Atomic Energy Commission.

(32) H. Haas and R. K. Sheline, *J. Chem. Phys.*, 47, 2996 (1967).

(33) L. H. Jones, "Advances in the Chemistry of Coordination Compounds," S. Kirschner, Ed., Macmillan, New York, N. Y., 1961, p 348.

(34) The following stretch-bend interaction constants were allowed to vary and are judged to be the most significant.

	$Mn(CO)_5Br$		$Mn(CO)_6$	
i,j	$C_{i,j}$	$F_{i,j}$	$C_{i,j}$	$F_{i,j}$
D_{ax},γ	0.0388	−0.049	0.08	−0.051
D_{ax},ψ'	−0.12	0.20	−0.05	0.10
Δ,γ	−0.078	0.068	No equivalent	
Δ,ψ'	−0.09	0.09	No equivalent	

$C_{i,j}$ are in radian $mdyn^{-1}$; $F_{i,j}$ are in $radian^{-1}$ mdyn.